MICROSCOPY

Microscopy **62(4)**: 419–428 (2013)
doi: 10.1093/jmicro/dft037

Review

Extensive use of FRET in biological imaging

Yoshiyuki Arai[1] and Takeharu Nagai[1,2,*]

[1]The Institute of Scientific and Industrial Research, Osaka University, 8-1 Mihogaoka, Ibaraki, Osaka 567-0047, Japan and [2]PRESTO, Japan Science and Technology Agency, Sanbancho, Chiyoda-ku, Tokyo 102-0075, Japan
*To whom correspondence should be addressed. E-mail: ng1@sanken.osaka-u.ac.jp

Abstract Förster resonance energy transfer (FRET) is a phenomenon used for bioimaging ranging from single molecules to *in vivo* scale. A large variety of organic dyes and fluorescent proteins are available for FRET probes. In this review, we introduce the representative pairs of FRET probes developed thus far. The efficiency of FRET is depending on the spectral overlap of donor emission and acceptor absorption, the orientation of donor and acceptor and their distance. For FRET-based indicators composed of fluorescent proteins, their orientation and dimeric property of donor and acceptor largely affect the FRET efficiency, indicating the effect for the performance of indicators. In addition, three major applications of FRET, including genetically encoded indicators, single-molecule FRET, and enhancement of chemiluminescent proteins, have been introduced and their functions have also been discussed.

Keywords FRET, fluorescent protein, orientation factor, single-molecule imaging

Received 29 April 2013, accepted 30 May 2013; online 23 June 2013

Introduction

A brief introduction to FRET

For many years, biologists have wanted to elucidate the events that occur in living systems, from the molecular level to the whole organ level. Optical imaging, and fluorescence imaging in particular, is a powerful technique because it allows us to visualize events occurring during the live state. Förster resonance energy transfer (FRET) is a physical phenomenon that can be applied for visualizing many biological events. FRET uses a pair of fluorophores and/or chromophores known as a donor and an acceptor. If the emission spectrum of the donor and the absorption spectrum of the acceptor overlap (Fig. 1a) and if the distance between the donor and the acceptor is close enough (typically, <10 nm) when the donor is excited by a light source or catalytic reaction, the excitation energy is transferred to the acceptor via a radiationless process. The characteristic distance, i.e. the so-called Förster distance (r_0), is calculated as follows:

$$r_0^6 = \frac{9000(\ln 10)\kappa^2 Q_D}{128\pi^5 N n^4} J(\lambda) \quad (1)$$

where κ^2 is the orientation factor that represents the geometric relationship between the donor emission transition dipole and acceptor absorption transition dipole, Q_D is quantum yield of the donor, N is Avogadro's number, n is the refractive index of the medium and $J(\lambda)$ is the overlap integral of normalized donor emission and acceptor absorption spectrum [1]. The energy transfer efficiency E is dependent on the inverse sixth power of the distance between the donor and acceptor molecules as follows:

$$E = \frac{r_0^6}{r^6 + r_0^6} \quad (2)$$

This equation tells us that if the distance between the donor and acceptor molecules is nearly r_0, a small

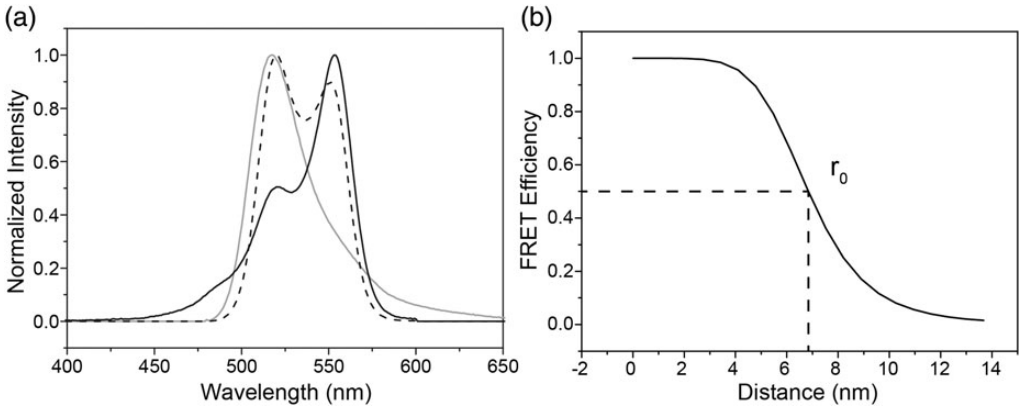

Fig. 1. (a) Spectrum overlap of donor emission (Alexa Flour®488 (Before this, Alexa Fluor®XXX is described as AlexaXXX), solid gray line), acceptor absorbance (Alexa555, solid black line) and overlap integral ($J(\lambda)$, dashed black line). (b) FRET efficiency according to the donor and acceptor distance. For Alexa488 and Alexa555 pairs, suppose $\kappa^2 = 2/3$ and the Förster distance is ~6.84 nm. If the donor and acceptor distance is equal to the Förster distance, FRET efficiency becomes 0.5.

change in the distance and geometrics dramatically affects the energy transfer efficiency (Fig. 1b) [1].

Pairs of donor and acceptor molecules

Currently, many organic dyes and fluorescent proteins have been developed and are being used as FRET donors and acceptors [2–4]. Table 1 shows representative FRET pairs categorized by organic dye-base, fluorescent protein base, hybrid of organic dye and fluorescent protein base, hybrid of organic and quantum dot (Qdot) base, and fluorescent and chemiluminescent protein base. FRET is mainly used in studies for investigating molecular interactions and conformational changes in biomolecules. In addition, FRET can be applied to develop indicators for biological functions as well as to enhance chemiluminescent signals and near-infrared probes for living organisms. Fluorescent protein pairs have been used to visualize molecular interactions in live cells, whereas organic dyes are preferentially used for *in vitro* studies, especially for single-molecule experiments, because they have higher photostability than fluorescent proteins. Fortunately, due to the enormous contribution of many researchers, now we can choose many FRET pairs which suit for one's purpose. For intra-molecular FRET, r_0 values should be considered to increase the dynamic range of FRET efficiency. In both cases, separation of spectrum of donor and acceptor is important to obtain better FRET data. Spectral unmixing techniques will contribute to extract donor and acceptor emission dramatically [5].

Development of FRET-based indicators to sense biological molecular processes; the importance of geometric orientation, dimerization properties and linker length

FRET-based indicators are excellent tools for sensing concentrations of target molecules and activities of protein in living cells. For sensing purposes, the basic structure was observed using yellow cameleon (YC), which was developed by Miyawaki *et al.* [6]. Cyan fluorescent protein (CFP) as a donor and yellow fluorescent protein (YFP) as an acceptor were connected via a Ca^{2+}-binding domain, calmodulin (CaM), and an M13 peptide, which is derived from skeletal muscle myosin light chain kinase and can bind to the Ca^{2+}-bound form of CaM. Upon Ca^{2+} binding, the conformation of CaM and M13 are compacted, and the distance between CFP and YFP becomes short, leading to efficient FRET from CFP to YFP. This genetically encoded Ca^{2+} indicator (GECI) is a powerful tool for Ca^{2+} imaging in specific cells and the cellular compartment, such as the mitochondria, nucleus and endoplasmic reticulum, because organic Ca^{2+} indicators, such as Fura2, X-Rhod and Fluo4 [7,8], have no targetability. Though the first version of YC successfully detected the Ca^{2+} concentration, its dynamic range was small [6]. What were the problems with this method? One of the possibilities was the orientation factor. As shown in Eqs. (1) and (2), the efficiency of FRET is closely dependent on not only the distance between the donor and acceptor but also the relative orientation of the transition dipole moment of donor emission and acceptor absorption, which is described as

Table 1. Pairs of FRET probes

Donor	Acceptor	Excitation wavelength (nm)	Emission wavelength of donor (nm)	Emission wavelength of acceptor (nm)	r_0 (nm)	Application	References
Sirius	mseCFP	370	435	479	3.7	SCAT3 indicator	[41]
BFP	GFP (C-S65T)	380	460	540	4.1	Protein dynamics cAMP indicator	[42,43]
T-Sapphire	mOrange	399	450–590	540–660	n/d	Intermolecular interaction	[44]
mAmetrine	tdTomato	406	526	581	n/d	Caspase-3 indicator	[45]
T-Sapphire	PSmOrange2	415	480	575	n/d	Photoswitching probes	[46]
mCellurian	mCitrine	420	470	535	n/d	cAMP indicator	[47]
mTurquoise	eYFP (cpVenus)	420	470	535	5.7	G Protein indicator	[38,40,48]
eCFP	tdTomato	433	470–530	570–670	n/d	cAMP sensor	[49]
eCFP	mDsRed	433	475	580	4.17	Tandem use	[50]
eCFP	YPet	433	475	530	n/d	Src, PKA, ERK biosensor	[51–53]
CyPet	YPet	435	477	530	n/d	Protein dynamics	[21,51]
LSSmOrange	LSSmKate2	437	572	605	n/d	FCCS, multicolor FRET	[54]
CFP	YFP, cpVenus	457	480	520	4.7–4.90	Ca^{2+} indicator, G protein indicator	[6,12,16,39,41,55]
mseCFP	PA-GFP	458	465–510	510–600	4.1	Photo-activatable probes	[56,57]
mTFP1	mCitrine	462	488	529	5.7	Caspase-3 indicator, H3K27-trimethylation biosensor	[45,58,59]
GFP	TMR	470	510	610	5.3	Protein–protein interaction	[60]
GFP	Alexa546	480	508	568	5.1	Rac activation indicator	[61]
Alexa488	Alexa594	485	515	620	6.0	Protein dynamics	[17,62,63]
Alexa488	TMR	488	520	610	6.1	Protein–protein interaction	[63,64]
eGFP	mDsRed	488	507	580	4.73	Tandem use	[50,55]
eGFP	mRFP	488	510	600	4.7	With use of FLIM	[65]
sYFP2	mRFP	488	505–550	585 long pass	5.6	With use of FLIM	[66]
TagGFP	TagRFP	488	500–530	560–600	5.74	With use of FLIM	[67]
Clover	mRuby2	505	515	600	6.3	CaMKIIa indicator	[68]
Cy3	Atto647N	515	535–800	635–800	6.7	DNA dynamics	[20]
TMR	Atto647	515	535–800	635–800	6.7	DNA dynamics	[20]
TMR	Cy5	515	535–800	635–800	6.5	DNA dynamics	[20,22]
TMR	IC5	515	575	680	5.8	Protein dynamics	[19]
Cy3	Cy5	514.5or 532	580	660	5.4	Molecular dynamics	[18,20,23]
mKO	mCherry	515	505–550	585 long pass	6.4	With use of FLIM	[66]
tagRFP	mPlum	542	593	649	n/d	Ras activation indicator	[69,70]
mOrange2	mKate2	549	573	644	n/d	Monosaccaride indicator	[71]
mOrange	mCherry	561	565–600	610–650	6.3	ORNEX4 (Annexin A4 indicator)	[66,72]
Qdot510, Qdot530, Qdot555,	Cy3	430	510, 530, 555	570	4,73, 5.04, 5.65	Qdot-based FRET demonstration	[73]
QDot525	Cy3	405	525	570	n/d	High-concentration TIRF imaging	[31]
Cybate	Cypate	720	760	810	6.13	NIR-caspase 3 indicator	[74]
MMPSense 750 FAST	MMPSense 750 FAST	740	755–900	755–900	n/d	NIR-cancer probes	[75]
mTFP1	eYFP	770 (2-photon)	480	520	n/d	With use of FLIM	[76]
eGFP	mStrawberry	960 (2-photon)	535	596	n/d	With use of FLIM	[76,77]
RLuc	EYFP	coelenterazine	480	520	5.0	Enhancement of chemiluminescence	[78]
RLuc8	EYFP	coelenterazine	480	520	n/d	Enhancement of chemiluminescence	[79]
RLucX	Venus	coelenterazine	480	520	n/d	Enhancement of chemiluminescence	[36]

κ^2, as given below:

$$\kappa^2 = (\cos\theta_T - 3\cos\theta_D \cos\theta_A)^2 \quad (3)$$

where θ_T is the angle between the emission transition dipole of the donor and the absorption transition dipole of the acceptor, θ_D and θ_A are the angle of these dipoles against the vector joining donor and acceptor [1]. The κ^2 value takes on 0–4 values corresponding to the orientations of the donor emission transition dipole and acceptor absorption transition dipole from perpendicular to parallel. As shown in Fig. 2, the r_0 value largely changes upon the κ^2 value changing. This means that even when the distance between donor and acceptor is constant, changes in orientation should affect the FRET efficiency.

In most cases, the κ^2 value is assumed to be 2/3, meaning that the donor and acceptor freely rotate during donor excitation life time, and thus, the dipole orientation should be isotropic [9]. This may be true in cases using small organic dyes because of their small size [10], showing almost zero fluorescence anisotropy. However, since the size of fluorescent proteins is sufficiently large (~3 nm) and the shape of the conformation is not globular but barrel-like, the orientations of fluorescent proteins are relatively hindered. Indeed, fluorescence anisotropy of fluorescent proteins in living cells is around 0.2 [11]. Thus, the orientation of fluorescent proteins in GECIs should be arranged. Nagai *et al.* invented a method to rigorously change the dipole orientation in an FRET-based GECI, YC. Several circularly permuted Venus fluorescent proteins (cpVenus) were created, and the Venus in YC was replaced with the cpVenus (Fig. 3). Among the constructs, YC3.60, which has cp173Venus as the acceptor, showed almost 90% FRET efficiency in the Ca^{2+}-bound form, resulting in the biggest dynamic range (600%) [12]. Expectedly, the fluorescence anisotropy in YC3.60 dramatically decreased from 0.12 to −0.05 because of the fluorescence depolarization upon Ca^{2+} binding [12].

Another important factor to increase FRET efficiency (i.e. increase the dynamic range) is the dimerization properties of fluorescent proteins. Since the concentration of transiently expressed protein in living cells is at the micromolar level and the dissociation constant of native *Aequorea* GFP (aqGFP) is ~74 μM, the monomeric version of aqGFP is in fact preferred for bioimaging [13]. The mutation A206K in aqGFP causes a complete monomeric phenotype (the K_d cannot be determined), and this mutant also works for other aqGFP color variants. As shown in Table 1, many types of monomeric proteins can be used as the FRET donor and acceptor. However, the formation of the 'complete monomer' may result in repulsion derived from the positive charge of the lysine residue, which may inhibit the close interaction of FRET pair of proteins. Kotera *et al.* examined which 'monomeric' or 'native' property works well as an FRET-based indicator in order to develop sensors with high dynamic ranges [14]. They found that the FRET efficiency increased when 'native' fluorescent proteins were used. Although the 'dimerization' mutant S208F/V224L also increased the FRET efficiency, due to the high dimerization properties of this mutant, FRET occurred even in the

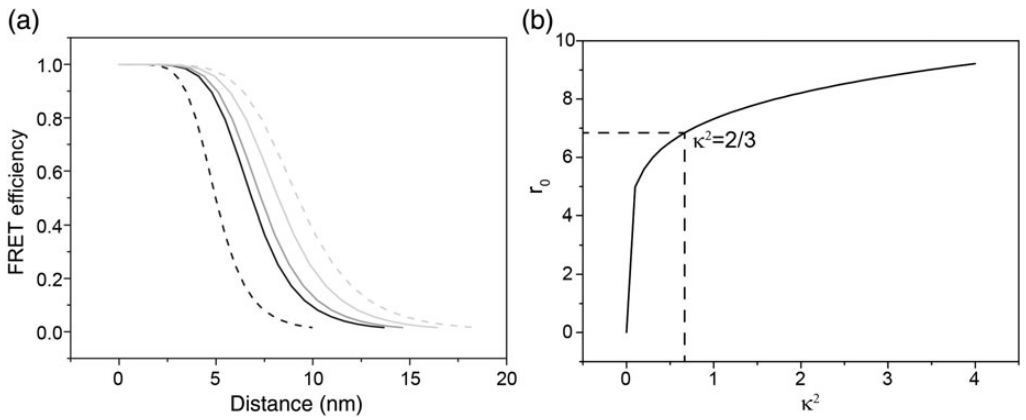

Fig. 2. (a) FRET efficiency for different κ^2 values = 0.1 (dashed black line), 2/3 (solid black line), 1.0 (solid gray line), 2.0 (solid light gray line) and 4.0 (dashed light gray line) for Alexa488 and Alexa555 pairs. (b) Relationship between κ^2 value and Förster distance (r_0). The relative orientation changes affect the r_0 value, leading to the change in FRET efficiency.

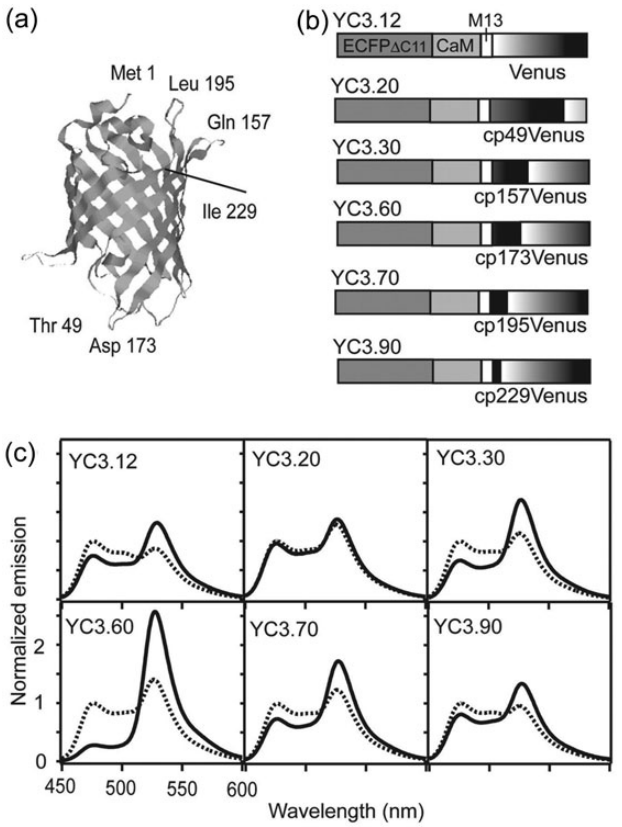

Fig. 3. Schematic structures and spectral properties of YC variants [12]. (a) The three-dimensional structure of GFP with the positions of the original (Met-1) and new N termini (Thr-49, Gln-157, Asp-173, Leu-195 and Ile-229) are indicated. (b) Domain structures of YC3.12, YC3.20, YC3.30, YC3.60, YC3.70 and YC3.90. XCaM, Xenopus CaM; E104Q, mutation of the conserved bidentate glutamate (E104) at position 12 of the third Ca^{2+}-binding loop to glutamine. (c) Emission spectra of YC variants (excitation at 435 nm) at zero (dotted line) and saturated Ca^{2+} (solid line).

absence of the substrate, which also caused a low dynamic range because the FRET efficiency differences in the presence or in the absence of the substrate became small (Fig. 4). Therefore, 'native' aqGFP variant pairs give the highest dynamic range as indicators.

In addition, the K_d values for Ca^{2+} in a mixture of free CaM and free M13 were at the nanomolar level (4.85 nM) [15], whereas the K_d values for the YC series were in the order of several hundred nanomolars (e.g. 250 nM in YC3.60) [12]. Therefore, there is the probability of steric hindrance for sensor domains inhibiting the binding of substrate. To improve the binding affinity, Horikawa *et al.* screened the optimal linker length between CaM and M13 [16]. They succeeded in the construction of the YC with the highest reported binding affinity, which was named 'YC-nano' and had K_d values ranging from 15 to 60 nM. These probes enabled the detection of the intrinsic activity of neuronal cells and oscillative signal propagation during cellular aggregation of *Dictyostelium discoideum* [16].

Compatible use of FRET and single-molecule imaging

Because FRET senses distance changes of <10 nm, the FRET measurement is a powerful technique for analysis of RNA, DNA and protein dynamics [17–23]. Furthermore, the compatible use of FRET and single-molecule imaging enables us to observe real-time conformational changes in individual molecules [24]. Zhuang *et al.* labeled ribozymes with Cy3 and Cy5 and measured the reaction rate by observing real-time conformational changes during catalytic reactions [23]. Ribozymes showed four different docked and undocked states with different rate constants. They found that there exists a strong 'memory effect' in that individual ribozymes prefer a certain rate constant.

The study of this 'memory effect' for individual molecules has been reported by Lu *et al.* for flavine adenine dinucleotide (FAD) [25]. The catalytic rate constant of single FAD molecules for its substrate flavin did not exhibited static rate constant, but indicated dynamic behavior that the rate constant followed time-dependent process, called dynamic disorder. This dynamic disorder indicates the individuality of molecules. Other proteins have also been shown to have such a memory effect [26,27]. Taken together, these results demonstrated that single-molecule FRET has provided new insights into molecular dynamics. However, the data analysis technique is still immature because of the challenge of how to treat noisy signals. Recently, Terentyeva *et al.* reported that inappropriate treatment of data for single-molecule FRET data has caused misunderstandings of the physiological meaning of its phenomena [28].

Blinking of fluorophores, which is unique for single-molecule observations, is a major issue for compatible use of FRET and single-molecule imaging. The excited state of the fluorophore transits to the basal state through radiative or nonradiative processes during the fluorescence lifetime. However, the excited-state fluorophore sometimes transits to the triplet states, which has microsecond fluorescence lifetime, leading to the late photon-emitting rate.

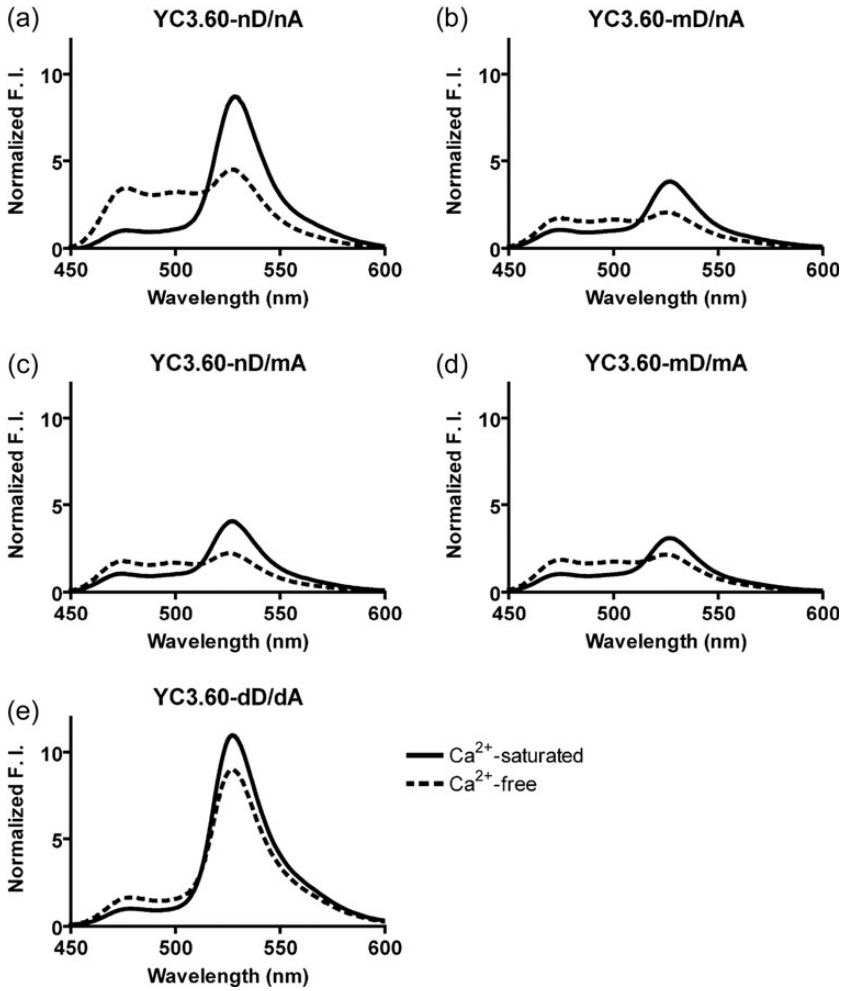

Fig. 4. Fluorescence spectra of cameleon YC3.60 variants [14]. (a) The original cameleon YC3.60-nD/nA. Variants with monomer-associated mutants (b) YC3.60-mD/nA, (c) YC3.60-nD/mA, (d) YC3.60-mD/mA and (e) with the dimer-enhanced mutant YC3.60-dD/dA in Ca^{2+}-saturated (solid curves) and Ca^{2+}-free (dotted curves) buffer. The spectra are normalized to the CFP peak in Ca^{2+}-saturated buffer. F.I. = fluorescence intensity.

Repeated cycling between the emitting and late photon-emitting states is observed, similar to when stars blink because of fluctuation in the atmosphere; this phenomenon is called blinking. If the blinking occurs in an acceptor, the apparent FRET efficiency is low, which results in misleading data analysis. To solve these problems, Lee *et al.* developed a measurement system named ALEX (alternating laser excitation) [29]. In this system, the donor and acceptor are alternately excited by lasers. The direct excitation of acceptor molecules provides information regarding the state of the acceptor, that is, whether it is in the photon-emitting or nonphoton-emitting state. Kozuka *et al.* also performed a similar alternating excitation of donor and acceptor fluorophores to monitor the acceptor states [19].

Another interesting FRET technique is the use of the donor as nano-sized light source. Evanescent fields evoked by total internal reflection of excitation light enable the excitation of only the fluorophores located near a glass surface (within about 200 nm), reducing the background fluorescence noise dramatically [30]. However, even with the use of evanescent field light excitation, the concentration of the fluorophores is limited to about 10 nM because the background fluorescence signal increases on the excitation of so many fluorescent molecules. FRET was used to overcome this limitation. Sugawa *et al.* attached quantum dots (Qdots) as donors to the myosin molecules [31]. As an acceptor, Cy3-labeled ATP (Cy3-ATP) was used to observe ATP catalytic events. On using FRET, Cy3 signals were observed

only near the Qdot surface, which meant that the fluorescent signals indicated the binding of Cy3–ATP to myosin. They succeeded in increasing the concentration of Cy3–ATP up to 10 μM, which was three orders higher than that achievable by evanescent field-based illumination.

Currently, FRET is used for super-resolution imaging, which breaks the Abbe's diffraction limit. Bates *et al.* found that Cy3–Cy5 pairs can be switched on and off by red light illumination [32]. By using weak red light, FRET signals can be modulated stochastically. If the fluorescent probes are activated stochastically and emit enough photons, we can easily determine their center position in nanometer accuracy [33]. One of the super-resolution techniques, called stochastic optical reconstruction microscopy (STORM), is based on this technique. Because there are a lot of pairs of FRET fluorophores available, multicolor super-resolution imaging is easily achieved by STORM [34].

Improvement of the brightness of chemiluminescent proteins

FRET can also be used to enhance weak donor fluorescence. *Renilla* luciferase (RLuc) is one such chemiluminescent protein that emits blue luminescence by catalyzing the oxidation of coelenterazine to yield celenteramide. The luminescence quantum yield of RLuc is quite low (approximately 0.05). However, if the chemiluminescent protein is located within a short distance from the fluorescent protein, which has a high fluorescence quantum yield, the excitation energy of the chemiluminescent protein is transferred to the fluorescent protein, leading to high photon emission. Indeed, the sea pansy *Renilla reniformis* can emit green fluorescence itself because FRET occurs between RLuc and *Renilla* green fluorescent proteins (RGFPs) with a surprising ~100% FRET efficiency [35]. By mimicking this natural system, Saito *et al.* developed the brightest FRET-based chemiluminescent protein, named Nano-lantern, which enabled video-rate imaging of cancer cells in a freely moving unshaved mouse [36]. They also developed a series of the sensors for Ca^{2+}, ATP and cAMP, inserting the sensor domain for each of these molecules into the RLuc moiety of Nano-lantern. Because Nano-lantern-based probes do not require excitation light, innate problems in fluorescence observation, such as autofluorescence and phototoxicity, can be avoided. In addition, Nano-lantern and Nano-lantern-based indicators are highly compatible with optogenetic tools such as ChR2 and NpHR. If fluorescent proteins or fluorescent protein-based indicators are used in conjunction with optogenetic tools, the excitation light for fluorescence observation must misactivate optogenetic tools [37].

Conclusions

FRET has become an essential technology for biologists. We hope that the FRET pairs shown in Table 1 will help to measure additional biological events. Conjugation of donor and acceptor proteins to sensor proteins may lead to improvements in novel fluorescence indicators. In addition, improving the orientation factor, native states of fluorescent proteins and linker length between the sensor domain and the donor and acceptor region will lead to an increase in FRET signals. Furthermore, the use of novel fluorescent proteins will also improve FRET signals. For example, CFP has been used as donor fluorescent protein. Recently, mTurquoise, a novel CFP developed from cerulean, can be replaced as a cyan donor [38–40]. For single-molecule FRET experiments, fluorescent dye's pairs help for long time observation of conformational fluctuations of molecules. However, specific labeling molecules by fluorescent dyes in cell are difficult. Compatible use of several tagging methods such as HaloTag™ technology, SNAP/CLIP tag technology and BL-tag technologies. Both chemiluminescent and near-infrared probes are extensively useful for *in vivo* imaging and the compatible use of optogeteic technique. The FRET technique also contributes to this important field. Therefore, FRET-based bioimaging techniques will become more powerful and more useful tools in the future.

Funding

This work was supported by a Grant-in-Aid for Scientific Research on Innovative Areas 'Spying minority in biological phenomena' (no. 3306) from MEXT (no. 23115003) (T.N.), Grant-in-Aid for Young Scientist (B) from Japan Society for the Promotion of Science (no. 23770168) (Y.A.), and PRESTO from Japan Science and Technology Agency (T.N.).

References

1 Lakowicz J R (2006) Energy transfer. In: Lakowicz J R (ed.), *Principles of Fluorescence Spectroscopy*, 3rd edn, pp. 443–475 (Springer, New York).

2 Shaner N C, Steinbach P A, and Tsien R Y (2005) A guide to choosing fluorescent proteins. *Nat. Methods* **2**: 905–909.

3 Panchuk-Voloshina N, Haugland R P, Bishop-Stewart J, Bhalgat M K, Millard P J, Mao F, and Leung W-Y (1999) Alexa dyes, a series of new fluorescent dyes that yield exceptionally bright, photostable conjugates. *J. Histochem. Cytochem.* **47**: 1179–1188.

4 Berlier J E, Rothe A, Buller G, Bradford J, Gray D R, Filanoski B J, Telford W G, Yue S, Liu J, Cheung C-Y, Chang W, Hirsch J D, Beechem Rosaria J M, Haugland P, and Haugland R P (2003) Quantitative comparison of long-wavelength Alexa Fluor dyes to Cy dyes: fluorescence of the dyes and their bioconjugates. *J. Histochem. Cytochem.* **51**: 1699–1712.

5 Zimmermann T, Rietdorf J, and Pepperkok R (2003) Spectral imaging and its applications in live cell microscopy. *FEBS Lett.* **546**: 87–92.

6 Miyawaki A, Llopis J, Heim R, and McCaffery J (1997) Fluorescent indicators for Ca^{2+} based on green fluorescent proteins and calmodulin. *Nature* **388**: 882–887.

7 Grynkiewicz G, Poenie M, and Tsien R Y (1985) A new generation of Ca^{2+} indicators with greatly improved fluorescence properties. *J. Biol. Chem.* **260**: 3440–3450.

8 Pologruto T A, Yasuda R, and Svoboda K (2004) Monitoring neural activity and [Ca^{2+}] with genetically encoded Ca^{2+} indicators. *J. Neurosci.* **24**: 9572–9579.

9 van der Meer B W (2002) Kappa-squared: from nuisance to new sense. *J. Biotechnol.* **82**: 181–196.

10 dos Remedios C G and Moens P D J (1995) Fluorescence resonance energy transfer spectroscopy is a reliable 'ruler' for measuring structural changes in proteins: dispelling the problem of the unknown orientation factor. *J. Struct. Biol.* **115**: 175–185.

11 Gautier I, Tramier M, Durieux C, Coppey J, Pansu R B, Nicolas J C, Kemnitz K, and Coppey-Moisan M (2001) Homo-FRET microscopy in living cells to measure monomer-dimer transition of GFP-tagged proteins. *Biophys. J.* **80**: 3000–3008.

12 Nagai T, Yamada S, Tominaga T, Ichikawa M, and Miyawaki A (2004) Expanded dynamic range of fluorescent indicators for Ca(2+) by circularly permuted yellow fluorescent proteins. *Proc. Natl Acad. Sci. USA* **101**: 10554–10559.

13 Zacharias D A, Violin J D, Newton A C, and Tsien R Y (2002) Partitioning of lipid-modified monomeric GFPs into membrane microdomains of live cells. *Science (New York, NY)* **296**: 913–916.

14 Kotera I, Iwasaki T, and Imamura H (2010) Reversible dimerization of *Aequorea victoria* fluorescent proteins increases the dynamic range of FRET-based indicators. *ACS Chem. Biol.* **5**: 215–222.

15 Martin S R, Bayley P M, Brown S E, Porumb T, Zhang M, and Ikura M (1996) Spectroscopic characterization of a high-affinity calmodulin-target peptide hybrid molecule. *Biochemistry* **35**: 3508–3517.

16 Horikawa K, Yamada Y, Matsuda T, Kobayashi K, Hashimoto M, Matsu-ura T, Miyawaki A, Michikawa T, Mikoshiba K, and Nagai T (2010) Spontaneous network activity visualized by ultrasensitive Ca(2+) indicators, yellow Cameleon-Nano. *Nat. Methods* **7**: 729–732.

17 Schuler B, Lipman E, and Eaton W (2002) Probing the free-energy surface for protein folding with single-molecule fluorescence spectroscopy. *Nature* **419**: 743–747.

18 Arai Y, Iwane A H, Wazawa T, Yokota H, Ishii Y, Kataoka T, and Yanagida T (2006) Dynamic polymorphism of Ras observed by single molecule FRET is the basis for molecular recognition. *Biochem. Biophys. Res. Commun.* **343**: 809–815.

19 Kozuka J, Yokota H, Arai Y, Ishii Y, and Yanagida T (2006) Dynamic polymorphism of single actin molecules in the actin filament. *Nat. Chem. Biol.* **2**: 83–86.

20 Di Fiori N and Meller A (2010) The effect of dye-dye interactions on the spatial resolution of single-molecule FRET measurements in nucleic acids. *Biophys. J.* **98**: 2265–2272.

21 Ohashi T, Galiacy S D, Briscoe G, and Erickson H P (2007) An experimental study of GFP-based FRET, with application to intrinsically unstructured proteins. *Protein Sci.* **16**: 1429–1438.

22 Sugawa M, Arai Y, Iwane A H, Ishii Y, and Yanagida T (2007) Single molecule FRET for the study on structural dynamics of biomolecules. *Bio Systems* **88**: 243–250.

23 Zhuang X, Kim H, Pereira M J B, Babcock H P, Walter N G, and Chu S (2002) Correlating structural dynamics and function in single ribozyme molecules. *Science (New York, NY)* **296**: 1473–1476.

24 Roy R, Hohng S, and Ha T (2008) A practical guide to single-molecule FRET. *Nat. Methods* **5**: 507–516.

25 Lu H P, Xun L, and Xie X S (1998) Single-molecule enzymatic dynamics. *Science (New York, NY)* **282**: 1877–1882.

26 English B P, Min W, van Oijen A M, Lee K T, Luo G, Sun H, Cherayil B J, Kou S C, and Xie X S (2006) Ever-fluctuating single enzyme molecules: Michaelis–Menten equation revisited. *Nat. Chem. Biol.* **2**: 87–94.

27 Yang H, Luo G, Karnchanaphanurach P, Louie T-M, Rech I, Cova S, Xun L, and Xie X S (2003) Protein conformational dynamics probed by single-molecule electron transfer. *Science (New York, NY)* **302**: 262–266.

28 Terentyeva T G, Engelkamp H, Rowan A E, Komatsuzaki T, Hofkens J, Li C-B, and Blank K (2012) Dynamic disorder in single-enzyme experiments: facts and artifacts. *ACS Nano* **6**: 346–354.

29 Lee N K, Kapanidis A N, Wang Y, Michalet X, Mukhopadhyay J, Ebright R H, and Weiss S (2005) Accurate FRET measurements within single diffusing biomolecules using alternating-laser excitation. *Biophys. J.* **88**: 2939–2953.

30 Takashi F, Yoshie H, Makio T, Kiwamu S, and Yanagida T (1995) Imaging of single fluorescent molecules and individual ATP turnovers by single myosin molecules in aqueous solution. *Nature* **374**: 555.

31 Sugawa M, Nishikawa S, Iwane A H, Biju V, and Yanagida T (2010) Single-molecule FRET imaging for enzymatic reactions at high ligand concentrations. *Small (Weinheim an der Bergstrasse, Germany)* **6**: 346–350.

32 Bates M, Blosser T, and Zhuang X (2005) Short-range spectroscopic ruler based on a single-molecule optical switch. *Phys. Rev. Lett.* **94**: 1–4.

33 Yildiz A, Forkey J N, McKinney S A, Ha T, Goldman Y E, and Selvin P R (2003) Myosin V walks hand-over-hand: single fluorophore imaging with 1.5-nm localization. *Science (New York, NY)* **300**: 2061–2065.

34 Bates M, Huang B, Dempsey G T, and Zhuang X (2007) Multicolor super-resolution imaging with photo-switchable fluorescent probes. *Science (New York, NY)* **317**: 1749–1753.

35 Ward W W and Cormier M J (1976) In vitro energy transfer in Renilla bioluminescence. *J. Phys. Chem.* **80**: 2289–2291.

36 Saito K, Chang Y-F, Horikawa K, Hatsugai N, Higuchi Y, Hashida M, Yoshida Y, Matsuda T, Arai Y, and Nagai T (2012) Luminescent proteins for high-speed single-cell and whole-body imaging. *Nat. Commun.* **3**: 1262.

37 Nagel G, Szellas T, Huhn W, Kateriya S, Adeishvili N, Berthold P, Ollig D, Hegemann P, and Bamberg E (2003) Channelrhodopsin-2, a directly light-gated cation-selective membrane channel. *Proc. Natl Acad. Sci. USA* **100**: 13940.

38 Markwardt M L, Kremers G-J, Kraft C A, Ray K, Cranfill P J C, Wilson K A, Day R N, Wachter R M, Davidson M W, and Rizzo M A (2011) An improved cerulean fluorescent protein with enhanced brightness and reduced reversible photoswitching. *PloS One* **6**: e17896.

39 Janetopoulos C, Jin T, and Devreotes P (2001) Receptor-mediated activation of heterotrimeric G-proteins in living cells. *Science (New York, NY)* **291**: 2408–2411.

40 Adjobo-Hermans M J W, Goedhart J, van Weeren L, Nijmeijer S, Manders E M M, Offermanns S, and Gadella T W J (2011) Real-time visualization of heterotrimeric G protein Gq activation in living cells. *BMC Biol.* **9**: 32.

41 Tomosugi W, Matsuda T, Tani T, Nemoto T, Kotera I, Saito K, Horikawa K, and Nagai T (2009) An ultramarine fluorescent protein with increased photostability and pH insensitivity. *Nat. Methods* **6**: 351–353.

42 Philipps B, Hennecke J, and Glockshuber R (2003) FRET-based in vivo screening for protein folding and increased protein stability. *J. Mol. Biol.* **327**: 239–249.

43 Zaccolo M, De Giorgi F, Cho C Y, Feng L, Knapp T, Negulescu P A, Taylor S S, Tsien R Y, and Pozzan T (2000) A genetically encoded, fluorescent indicator for cyclic AMP in living cells. *Nat. Cell Biol.* **2**: 25–29.

44 Bayle V, Nussaume L, and Bhat R A (2008) Combination of novel green fluorescent protein mutant TSapphire and DsRed variant mOrange to set up a versatile in planta FRET-FLIM assay. *Plant Physiol.* **148**: 51–60.

45 Ai H, Hazelwood K, Davidson M, and Campbell R (2008) Fluorescent protein FRET pairs for ratiometric imaging of dual biosensors. *Nat. Methods* **5**: 401–403.

46 Subach O M, Entenberg D, Condeelis J S, and Verkhusha V V (2012) A FRET-facilitated photoswitching using an orange fluorescent protein with the fast photoconversion kinetics. *J. Am. Chem. Soc.* **134**: 14789–14799.

47 Salonikidis P S, Niebert M, Ullrich T, Bao G, Zeug A, and Richter D W (2011) An ion-insensitive cAMP biosensor for long term quantitative ratiometric fluorescence resonance energy transfer (FRET) measurements under variable physiological conditions. *J. Biol. Chem.* **286**: 23419–23431.

48 Klarenbeek J B, Goedhart J, Hink M A, Gadella T W J, and Jalink K (2011) A mTurquoise-based cAMP sensor for both FLIM and ratiometric read-out has improved dynamic range. *PloS One* **6**: e19170.

49 Van Der Krogt G N M, Ogink J, Ponsioen B, Jalink K, and van der Krogt G N M (2008) A comparison of donor-acceptor pairs for genetically encoded FRET sensors: application to the Epac cAMP sensor as an example. *PloS One* **3**: e1916.

50 Erickson M G, Moon D L, and Yue D T (2003) DsRed as a potential FRET partner with CFP and GFP. *Biophys. J.* **85**: 599–611.

51 Nguyen A W and Daugherty P S (2005) Evolutionary optimization of fluorescent proteins for intracellular FRET. *Nat. Biotechnol.* **23**: 355–360.

52 Ouyang M, Sun J, Chien S, and Wang Y (2008) Determination of hierarchical relationship of Src and Rac at subcellular locations with FRET biosensors. *Proc. Natl Acad. Sci. USA* **105**: 14353–14358.

53 Komatsu N, Aoki K, Yamada M, Yukinaga H, Fujita Y, Kamioka Y, and Matsuda M (2011) Development of an optimized backbone of FRET biosensors for kinases and GTPases. *Mol. Biol. Cell* **22**: 4647–4656.

54 Shcherbakova D M, Hink M A, Joosen L, Gadella T W J, and Verkhusha V V (2012) An orange fluorescent protein with a large Stokes shift for single-excitation multicolor FCCS and FRET imaging. *J. Am. Chem. Soc.* **134**: 7913–7923.

55 Patterson G H, Piston D W, and Barisas B G (2000) Förster distances between green fluorescent protein pairs. *Anal. Biochem.* **284**: 438–440.

56 Demarco I, Periasamy A, Booker C, and Day R (2006) Monitoring dynamic protein interactions with photoquenching FRET. *Nat. Methods* **3**: 519–524.

57 Matsuda T, Miyawaki A, and Nagai T (2008) Direct measurement of protein dynamics inside cells using a rationally designed photoconvertible protein. *Nat. Methods* **5**: 339–345.

58 Ibraheem A, Yap H, Ding Y, and Campbell R E (2011) A bacteria colony-based screen for optimal linker combinations in genetically encoded biosensors. *BMC Biotechnol.* **11**: 105.

59 Ai H, Henderson J N, Remington S J, and Campbell R E (2006) Directed evolution of a monomeric, bright and photostable version of Clavularia cyan fluorescent protein: structural characterization and applications in fluorescence imaging. *Biochem. J.* **400**: 531–540.

60 Zoffmann S, Bertrand S, Do Q-T, Bertrand D, Rognan D, Hibert M, and Galzi J-L (2007) Topological analysis of the complex formed between neurokinin A and the NK2 tachykinin receptor. *J. Neurochem.* **101**: 506–516.

61 Kraynov V S, Chamberlain C, Bokoch G M, Schwartz M A, Slabaugh S, and Hahn K M (2000) Localized Rac activation dynamics visualized in living cells. Science (New York, NY*)* **290**: 333–337.

62 Botelho A V, Huber T, Sakmar T P, and Brown M F (2006) Curvature and hydrophobic forces drive oligomerization and modulate activity of rhodopsin in membranes. *Biophys. J.* **91**: 4464–4477.

63 Frederix P and Asselbergs M (2001) High sensitivity spectrograph for use in fluorescence microscopy. *Appl. Spectrosc.* **55**: 1005–1012.

64 Koch H P, Kurokawa T, Okochi Y, Sasaki M, Okamura Y, and Larsson H P (2008) Multimeric nature of voltage-gated proton channels. *Proc. Natl Acad. Sci. USA* **105**: 9111–9116.

65 Peter M, Ameer-Beg S M, Hughes M K Y, Keppler M D, Prag S, Marsh M, Vojnovic B, and Ng T (2005) Multiphoton-FLIM quantification of the EGFP-mRFP1 FRET pair for localization of membrane receptor-kinase interactions. *Biophys. J.* **88**: 1224–1237.

66 Goedhart J, Vermeer J E M, Adjobo-Hermans M J W, van Weeren L, and Gadella T W J (2007) Sensitive detection of p65 homodimers using red-shifted and fluorescent protein-based FRET couples. *PloS One* **2**: e1011.

67 Shcherbo D, Souslova E A, Goedhart J, Chepurnykh T V, Gaintzeva A, Shemiakina I I, Gadella T W J, Lukyanov S, and Chudakov D M (2009) Practical and reliable FRET/FLIM pair of fluorescent proteins. *BMC Biotechnol.* **9**: 24.

68 Lam A J, St-Pierre F, Gong Y, Marshall J D, Cranfill P J, Baird M A, McKeown M R, Wiedenmann J, Davidson M W, Schnitzer M J, Tsien R Y, and Lin M Z (2012) Improving FRET dynamic range with bright green and red fluorescent proteins. *Nat. Methods* **9**: 1005–1012.

69 Grant D M, Zhang W, McGhee E J, Bunney T D, Talbot C B, Kumar S, Munro I, Dunsby C, Neil M A A, Katan M, and French P M W (2008) Multiplexed FRET to image multiple signaling events in live cells. *Biophys. J.* **95**: L69–L71.

70 Wang L, Jackson W C, Steinbach P A, and Tsien R Y (2004) Evolution of new nonantibody proteins via iterative somatic hypermutation. *Proc. Natl Acad. Sci. USA* **101**: 16745–16749.

71 Bourdès A, Rudder S, East A K, and Poole P S (2012) Mining the *Sinorhizobium meliloti* transportome to develop FRET biosensors for sugars, dicarboxylates and cyclic polyols. *PLoS One* **7**: e43578.

72 Piljic A and Schultz C (2008) Simultaneous recording of multiple cellular events by FRET. *ACS Chem. Biol.* **3**: 156–160.

73 Clapp A and Medintz I (2004) Fluorescence resonance energy transfer between quantum dot donors and dye-labeled protein acceptors. *J. Am. Chem. Soc.* **126**: 301–310.

74 Zhang Z, Fan J, Cheney P P, Berezin M Y, Edwards W B, Akers W J, Shen D, Liang K, Culver J P, and Achilefu S (2009) Activatable molecular systems using homologous near-infrared fluorescent probes for monitoring enzyme activities in vitro, in cellulo, and in vivo. *Mol. Pharm.* **6**: 416–427.

75 Solomon M, Guo K, Sudlow G P, Berezin M Y, Edwards W B, Achilefu S, and Akers W J (2011) Detection of enzyme activity in orthotopic murine breast cancer by fluorescence lifetime imaging using a fluorescence resonance energy transfer-based molecular probe. *J. Biomed. Optics* **16**: 066019.

76 Padilla-Parra S, Audugé N, Lalucque H, Mevel J-C, Coppey-Moisan M, and Tramier M (2009) Quantitative comparison of different fluorescent protein couples for fast FRET-FLIM acquisition. *Biophys. J.* **97**: 2368–2376.

77 Shu X, Shaner N, and Yarbrough C (2006) Novel chromophores and buried charges control color in mFruits. *Biochemistry* **45**: 9639–9647.

78 Xu Y, Piston D, and Johnson C (1999) A bioluminescence resonance energy transfer (BRET) system: application to interacting circadian clock proteins. *Proc. Natl Acad. Sci. USA* **96**: 151–156.

79 Hoshino H, Nakajima Y, and Ohmiya Y (2007) Luciferase-YFP fusion tag with enhanced emission for single-cell luminescence imaging. *Nat. Methods* **4**: 637–639.